

## Two-Photon Excited Molecular Fluorescence

M. J. WIRTH<sup>1</sup> and F. E. LYTTLE

Department of Chemistry, Purdue University, West Lafayette, IN 47907

A two-fold approach is taken in the investigation of the analytical aspects of two-photon spectroscopy. A novel laser source is introduced and characterized as an expedient means of achieving two-photon absorption; and two-photon excited fluorescence spectroscopy is demonstrated as a promising method for chemical analysis, with a diversity of applications.

The high peak power and continuous nature of the synchronously pumped cw dye laser allows the generation of a sensitive and precise two-photon excitation response, and the wide tunability range allows acquisition of two-photon excitation spectra. It has been determined that the cavity dumped version of the laser yields the best performance for two-photon spectroscopy and offers the most versatile output method.

The difference in selection rules for one- and two-photon spectroscopy gives rise to a complementary set of excitation spectra. Additionally, polarization information is retained in the two-photon excitation of randomly oriented molecules, therefore the excitation response can be selective with respect to the symmetry of the excited state. These features suggest the applicability of two-photon spectroscopy as a unique tool for qualitative analysis.

Since the wavelength of the incident radiation is twice that which corresponds to the transition, the two-photon excitation method can be used to probe species in optically dense media. It is demonstrated that fluorophors can be quantified in matrices having large and varying absorbances, with detection limits superior to those of one-photon spectroscopy. Also, the error due to reabsorption of emission can be minimized by utilizing the spatial selectivity of the excitation process.

General Considerations. The term nonlinear optics refers to those phenomena involving light where the induced polarization,  $P$ , of an atomic or molecular electron cloud is not at the same

<sup>1</sup>Current address: Department of Chemistry, University of Wisconsin, Madison, WI 53706

frequency as that of the driving electric field strength,  $E$ . For a centrosymmetric molecule,  $P$  is related to  $E$  by the expression

$$P = \epsilon_0 \{ \chi_1 E + \chi_3 E^3 + \dots \} \quad \text{Eq. 1}$$

where  $\epsilon_0$  is the permittivity of free space and the  $\chi_i$  are the susceptibility tensors of order  $i$  and rank  $(i+1)$  (1).

Linear optics occurs when the susceptibilities are space and time independent, and when  $\chi_1 \gg \chi_3 \dots$ . For this situation Eq. 1 can be rewritten as

$$P_1(\omega) = \epsilon_0 \chi_1(\omega) E(\omega) \quad \text{Eq. 2}$$

where  $\omega$  is the frequency of the driving radiation. To describe the behavior of Eq. 2 at all frequencies, the susceptibility must be considered a complex quantity, i.e.,

$$\chi_1 = \chi_1' + i\chi_1'' \quad \text{Eq. 3}$$

At frequencies far removed from a transition resonance, the real part of Eq. 3 predominates. The resultant relationship between  $P$  and  $E$  contains a phase lag which is experimentally observed as the refractive index, where  $n^2 = 1 + \chi_1'$ . At frequencies near resonance the imaginary part predominates. The electric field is then absorbed to an extent determined by the extinction coefficient,  $k$  where  $2nk = \chi_1''$ . The behavior of the system towards any given  $\omega$  will depend upon the relative magnitudes of  $\chi_1'(\omega)$  and  $\chi_1''(\omega)$ .

Non-linear Optics. The third order polarization of Eq. 1 can be expanded into the form

$$P_3(\omega_i) = \epsilon_0 \chi_3(\omega_i, \omega_j, \omega_k, \omega_l) E(\omega_j) E(\omega_k) E(\omega_l) \quad \text{Eq. 4}$$

where four waves are being mixed by  $\chi_3$ . Several common combinations of frequencies are shown in Table I. Like the first order polarization, the third order case exhibits important subcombinations that are identified by various resonance enhancements. Since these correspond to atomic or molecular transitions, the nonlinear effect can be used to obtain structural information.

The possibility of observing optical frequency nonlinear phenomena has long been established. An upper bound for the required field strength can be estimated by the field,  $E_0$ , binding an electron to the nuclei and the approximate rule that  $\chi_1/\chi_3 \sim E_0^2$  (2). A typical value for  $E_0$  would be  $3 \times 10^8 \text{ Vcm}^{-1}$  which corresponds to an intensity of  $\sim 10^{15} \text{ Wcm}^{-2}$ . The experimental dilemma was alleviated when in late 1960, T. Maiman published the design of the first laser (3). After this date nonlinear processes were discovered and/or verified in rapid succession - second harmonic generation (4) and two-photon absorption (5) in 1961; stimulated Raman scattering (6), sum and difference frequency generation (7),

Table I. Examples of Four Wave Mixing

Resultant Frequency	Mixed <sup>a</sup> Frequencies	Resonance <sup>b</sup> Frequency	Phenomenon
$3\omega_1$	$\omega_1, \omega_1, \omega_1$	---	Frequency tripling.
$\omega_1$	$\omega_1^*, \omega_1, \omega_1$	$\omega_1 = \omega_e$	Self-focusing. Self-induced transparency.
$\omega_2$	$\omega_1^*, \omega_1, \omega_2$	$\omega_1 + \omega_2 = \omega_e$ $\omega_1 - \omega_2 = \omega_v$ $\omega_2 - \omega_1 = \omega_v$	Intensity dependent refractive index. Two-photon absorption. Stimulated Raman emission. Inverse Raman absorption.
$2\omega_1 - \omega_2$	$\omega_1^*, \omega_1, \omega_2^*$	$\omega_1 - \omega_2 = \omega_v$	Four wave mixing. Coherent anti-Stokes Raman emission.

(a) The superscript star notation denotes that the complex conjugate of the electric field strength is utilized in the polarization equation.

(b)  $\omega_e$  = an electronic transition;  $\omega_v$  = a vibrational transition.

optical rectification (8), and frequency tripling (9) in 1962; self-focusing in 1964 (10); and coherent antiStokes Raman (CARS) generation in 1965 (11). Thus, much of the early work was involved with the understanding and prediction of these formerly unobserved effects.

Two-Photon Absorption. The third order susceptibility giving rise to two-photon absorption can be written as  $\chi_3(\omega_2, \omega_1, -\omega_1, \omega_2)$ . For this case the field strength product is written as  $E(\omega_1)E^*(\omega_1)E(\omega_2)$  or  $\bar{I}_1 E(\omega_2)$ , where  $\bar{I}_1$  is the cycle averaged intensity of  $\omega_1$ . The third order susceptibility can then be written as a correction term,  $\delta\chi$ , to the first order, where

$$\delta\chi_1(\omega_2) = \chi_3(\omega_2, \omega_1, -\omega_1, \omega_2) \bar{I}_1. \quad \text{Eq. 5}$$

The polarization at  $\omega_2$  then becomes

$$P(\omega_2) = \epsilon_0 \{ \chi_1(\omega_2) E(\omega_2) + \delta\chi_1(\omega_2) E(\omega_2) \} \quad \text{Eq. 6}$$

As long as  $\chi_1''$  and  $\delta\chi_1''$  are negligible,  $\omega_2$  will not be absorbed. This gives rise to an intensity dependent refractive index as the  $\delta\chi'$  term approaches the magnitude of  $\chi_1'$ . Whenever  $\chi_1'$  is large and positive, direct absorption of  $\omega_2$  occurs. Whenever,  $\delta\chi''$  is large and positive, an intensity dependent absorption of  $\omega_2$  occurs. Finally whenever  $\delta\chi_1''$  is large and negative, an intensity dependent stimulated emission of  $\omega_2$  occurs.

In the two-photon absorption process, an excited state is created with an energy twice that of the incident photons. The absorption law that the process obeys is similar to that for one-photon except that the absorption is intensity dependent, as predicted in the previous section. For small values, the fraction of light absorbed (12) can be determined by

$$\Delta P/P = [\delta P/A] \ell C \quad \text{Eq. 7}$$

where  $P$  is the incident power,  $\Delta P$  is the change in power due to absorption,  $\delta$  is the two-photon absorptivity,  $C$  is the concentration,  $\ell$  is the path length, and  $A$  is the transverse area of the incident beam. From equation 7 it is seen that the two-photon absorbance is proportional to concentration and path length as in Beer's law, and in addition it is proportional to the light intensity,  $P/A$ . Thus, the absorption can be enhanced by increasing the power or by focusing the beam more tightly. The laser parameter dependence makes measurements of absolute absorptions difficult.

A typical value for  $\delta$  is  $10^{-50} \text{ cm}^4 \text{ s photon}^{-1} \text{ molecule}^{-1}$ , which becomes  $10^{-11} \text{ L cm mole}^{-1} \text{ Watt}^{-1}$  for molar concentration and 333 nm radiation. The laser system used in this study could generate a 1 kW pulse and focus it to a 10  $\mu\text{m}$  spot. Thus, the two-photon cross-section,  $\delta P/A$ , is typically  $10^{-2} \text{ L mol}^{-1} \text{ cm}^{-1}$ ,

i.e., six orders of magnitude smaller than the corresponding one-photon cross-section.

The small magnitude of the cross-section is the basis of an experimental challenge in two-photon spectroscopy. Two-photon absorbance can be detected either by measuring the attenuation of the beam power, which is a relatively insensitive means, or by monitoring thermal, acoustical, ionization, or luminescence effects in the sample. In the reported work the response is monitored exclusively by fluorescence because of its sensitivity. From equation 7 it can be seen that the fluorescence intensity is proportional to  $\Delta P$ , and therefore to  $P^2$ .

### The Synchronously Pumped CW Dye Laser As A Source for Two-Photon Spectroscopy

The small magnitude of the absorption cross-section and the non-linear nature of the process, have required that pulsed laser sources be employed in two-photon spectroscopy in order to generate a measurable number of excited states. The usual difficulty with this method is that the excitation pulses vary unpredictably in amplitude, necessitating some means of correcting the measured response for laser pulse characteristics. Pulse height variations present a particularly severe problem in two-photon spectroscopy because the excitation depends upon the square of the incident power. This problem might be minimized by the use of continuous, mode-locked lasers because pulse fluctuations with these devices are small.

The synchronously pumped dye laser (SPDL) is a continuous, mode-locked laser with demonstrated ability to excite two-photon transitions (13). Pulse generation is achieved by matching the cavity length of the dye laser to that of the continuously mode-locked argon ion laser (14, 15, 16). Since mode-locking produces a train of pulses highly reproducible in amplitude and temporal profile, the peak power of each pulse is proportional to the average power of the train. Measurement of the average power of a continuous laser is straight forward and can be used to correct the measured two-photon excitation response for the incident peak power.

The Laser. The optical and electronic layout of the system is shown in Figure 1. A detailed description of the laser has been given previously by Harris et al. (14,17). A Coherent Radiation CR-6 argon-ion laser is mode-locked by a Coherent Radiation Model 464 acousto-optic modulator driven at 44 MHz, producing a continuous train of 0.4 ns wide pulses spaced 11 ns apart. This train is used to pump a Coherent Radiation Model 490 jet stream dye laser, the cavity length of which is adjusted to equal the pulse spacing. A Spectra-Physics Model 365 acousto-optic deflector is incorporated into the dye laser in order to dump pulses at a controlled rate. The synchronization between the mode-locked optical pulse circulating in the cavity and the deflector is

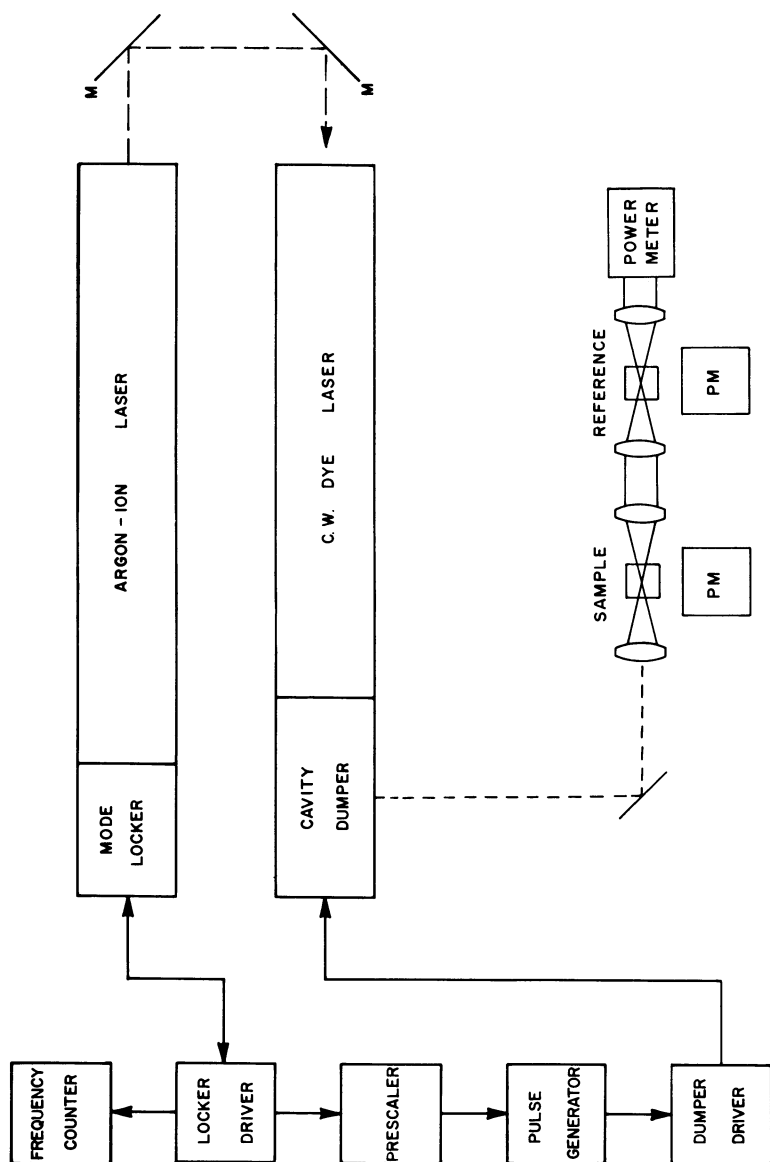


Figure 1. Optical and electronic block diagram of the two-photon fluorimeter. The components are described in the text.

provided by a high speed prescaler obtained from Electronic Digital Systems, Lafayette, Indiana. This unit provides a variable output rate ( $\sim 10$  MHz to  $\sim 5$  KHz) by activating a Hewlett-Packard Model 8013B pulse generator, which subsequently gates the 365 rf power. The dye laser was cavity dumped at repetition rates near 2 MHz to optimize the fluorescence intensity. The wavelength was monitored with a prism spectroscope having a precision of  $\sim 0.2$  nm.

Spectral Coverage. Three different dyes were used to obtain the fluorescence data, sodium fluorescein, rhodamine 6G, and rhodamine B. For the rhodamine dyes, all four mirrors in the dye laser cavity were coated for rhodamine 6G. For sodium fluorescein the pair of mirrors in the dye laser head were coumarin 6 mirrors and the dumper mirrors were coated for the argon-ion laser. The tuning curves for the dyes are given in Figure 2. From the figure it can be seen that the overall range of accessible wavelengths extends from 530 to 670 nm. Taking into account that the final states are one-half the wavelength of the incident beam, the effective tunability range extends from 265 to 325 nm. A wide variety of molecules have transitions in this spectral region, thus it is a useful working range for exploring the analytical possibilities of two-photon excited fluorescence spectroscopy.

In addition to the above dyes other groups have constructed sources based on a Krypton-ion laser and the dyes coumarin-102,-30 and -7 (18), and oxazine-1, DOTC and HITC (19). This gives a potential tuning range of 470-920 nm to access two-photon states between the wavelength limits of 235-460 nm.

Temporal Properties. The simplest experimental approach to obtaining two-photon spectra is to adjust the wavelength by rotation of the Lyot filter and to measure the resulting fluorescence intensity and laser power. After subtraction of a blank reading, the fluorescence intensity is normalized for the square of the incident power. Corrections of this type require that the shape of the picosecond pulses remain constant throughout the range of wavelengths. If the synchronously pumped laser is truly mode-locked, then the pulse shape will always remain constant. Mode-locked pulses are transform limited, meaning that the pulse width is the inverse of the spectral bandwidth of the lasing transition. Since the bandwidth is constant, the pulse width of a well mode-locked laser should remain fixed throughout the tuning range. In practice, however, the modulation in gain that causes mode locking is not perfect in that it is dependent upon the magnitude of the gain. Since the gain itself is wavelength dependent, it is expected that the pulse shapes will be altered at different points in the excitation spectra. Such changes in the output must be taken into account to obtain accurate two-photon excitation spectra.

There are two possible means of characterizing the two-photon response of the synchronously pumped laser: measuring the pulse width as a function of wavelength in order to calculate the actual

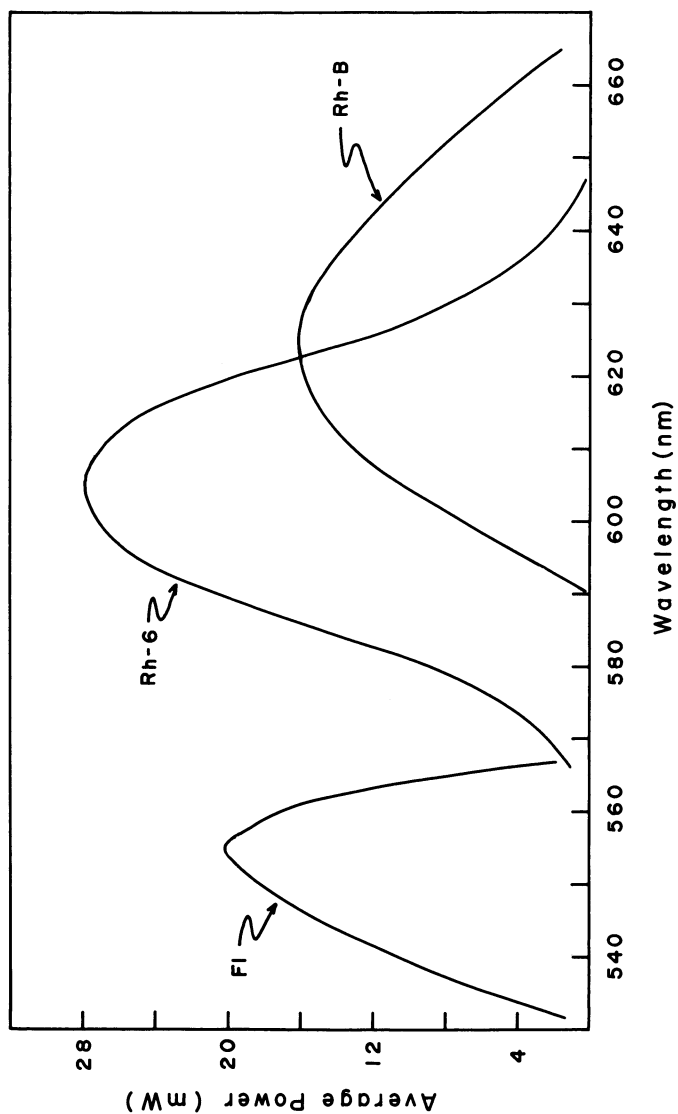


Figure 2. Tuning curves for the synchronously pumped dye laser. Fl, fluorescein; Rh-6, rhodamine 6G; and Rh-B, rhodamine B.



peak power; and generating the excitation spectrum of a known compound to obtain correction factors applicable to all successive spectra. Both methods were applied in the work to determine their relative merits.

The pulse width of the synchronously pumped dye laser has been reported as to be 10 ps or less (15,20,21,22). Thus it cannot be measured by any detector, with the possible exception of a streak camera. The usual method employed to measure such short pulse durations is an optical autocorrelation of the pulse train using a Michelson interferometer. The pulse profiles were measured in this work, under several laser conditions. The results of the interferometry showed that the pulses were transform limited only at very low gain. At high gains the pulses were not simply broadened, but actually were organized into two pulses. As a result an interferogram will be of limited utility in correcting excitation spectra because the pulse profiles are too complex to be reliable for determining the laser peak power. The information gained from this measurement supports the contention that the pulse shapes are not guaranteed to be uniform throughout the tuning range and there is definitely a need to correct for laser pulse shape variations in order to obtain the true excitation spectra.

The second approach for obtaining corrected excitation spectra is to generate a known spectrum to be used as a reference for all subsequent spectra. This method is limited by the ability to precisely determine the spectrum of the reference compound and can therefore introduce large uncertainties into the measurement. At present, however, it is a more practical means of correction than the pulse width measurement. It would be most convenient to use a reference compound with a fairly broad, structureless spectrum in order to maintain constant precision. In preliminary studies, several compounds were observed to have featureless spectra, and one compound in particular, bis-methylstyrylbenzene (bisMSB), appeared to be relatively flat throughout the rhodamine 6G range. The spectrum for the compound is shown in Figure 3a. Points that deviated from the curve were not reproducible from one spectrum to the next and were attributed to mismatches in the synchronous cavity length.

Rhodamine 6G has sufficiently large gain to allow cavity-dumped laser operation without mode-locking, thus affording the capability to scan the excitation spectrum with a well defined peak power. A bisMSB spectrum was corrected by this method and is shown in Figure 3b. The spectrum was measured to be flat to within 15%, indicating that the compound can serve as a useful reference. A comparison of the two spectra suggests that the pulse shape improves at the wings of the tuning range because the synchronously pumped laser generated spectrum exhibits over-corrections in this region.

### Qualitative Analysis Via Two-Photon Spectroscopy

The two-photon absorption process was first predicted in 1931 by Geoppart-Mayer (23) from recognizing that the Dirac theory for Raman scattering could be modified to describe the simultaneous absorption of two photons. Since the early 1960's, group theory and quantum mechanics have been exclusively used as tools to relate the measured absorptivity to the transition tensor in order to extract the characteristic molecular information. For electric dipole transitions in molecules possessing a center of symmetry, it has been shown that the parity of the excited state resulting from two-photon absorption is opposite to that from one-photon absorption (5). A two-photon spectrum would therefore reveal transitions due to gerade (even) states that are conventionally considered forbidden in electronic spectroscopy. This is analogous to the complementary relationship of infrared and Raman spectra.

Another unique feature of two-photon spectra is the presence of absorption peaks due to two electron transitions (24). In one-photon spectroscopy, the states connected by a transition may differ by only one orbital. In two-photon spectroscopy, since the intermediate state differs from the initial state by one orbital, then the final state may differ by two orbitals. The final state can therefore result from two promotions of one electron or one promotion of two electrons. The latter is strictly forbidden in one-photon spectroscopy.

A related area with analytical applicability is multiple photon ionization. Such methods typically employ a two-photon induced ionization, where selectivity is brought about by the presence of a resonant intermediate state to enhance the cross-section, and good detectability is achieved from the availability of sensitive detection methods for ions (25). A similar method is involved in the pursuit of isotope separation via multi-photon ionization. Efforts are concentrated in the infrared region where typically 30 or more photons are necessary for ionization. Studies are presently centered about the physics of the excitation process in order to understand the factors that determine the selectivity (26).

Two-Photon Transition Moment. For centrosymmetric molecules the one-photon transition only has significant oscillator strength when the parity of the electronic wave function changes upon absorption. This is because the electric dipole operator is an odd function, thus, in order for the transition moment to be nonzero, the states connected by the transition must have opposite parity (27). In most cases the ground state is the totally symmetric state and the energy levels detectable by one-photon spectroscopy correspond to the odd, or ungerade, states.

The two-photon absorption process can be thought of as two simultaneous one-photon absorptions, with the first photon

achieving an intermediate state and the second photon taking the molecule to the final state as shown in Figure 4. From this picture it can be ascertained that the two-photon excited state will be opposite in parity to the one-photon excited state. The transition moment is nonzero if the intermediate level has ungerade character and the final state is gerade. The two-photon spectrum will therefore be characteristic of the locations of the conventionally forbidden gerade states (5).

The intermediate state,  $|i\rangle$  can be considered an off-resonance level of all  $|u_k\rangle$ . This is possible since each  $|u_k\rangle$  could be described by a Lorentzian curve and thus extend to all frequencies. The transient nature of  $|i\rangle$  can be explained via the Heisenberg Uncertainty Principle, i.e., if  $E(u_k) - E(i) = 10,000 \text{ cm}^{-1}$ ,  $\Delta t$  is computed to be  $\sim 1 \text{ fsec}$ . This short lifetime requires that the photons interact simultaneously to produce the state  $|g_1\rangle$ .

The two photon transition moment between  $|g_0\rangle$  and  $|g_1\rangle$  can be written as

$$M(g_0, g_1) = \sum_k \left[ \frac{[e_1 \cdot M(g_0, u_k)][e_2 \cdot M(u_k, g_1)]}{E(u_k) - \hbar\omega_1} + \frac{[e_2 \cdot M(g_0, u_k)][e_1 \cdot M(u_k, g_1)]}{E(u_k) - \hbar\omega_2} \right] \quad \text{Eq. 8}$$

where  $M(g_0, u_k)$  and  $M(u_k, g_1)$  are the one-photon transition moments connecting the states  $|g_0\rangle$ ,  $|g_1\rangle$  and  $|u_k\rangle$ ,  $e_1$  and  $e_2$  are the polarization vectors of the two photons. A two-photon spectrum would consist of all  $j$  moments to even parity states.

Several characteristics of two-photon absorption can be inferred from Equation 8. First, as the energy of either photon approaches that of one of the  $|u_k\rangle$  states, the magnitude of the transition moment increases. Since the oscillator strength depends upon the square of the transition moment, this can provide a rather dramatic enhancement in the absorption cross-section. Again an analogy can be made with the Raman spectroscopy. Second, the summation is performed over all  $k$  ungerade states since  $|i\rangle$  is considered to be an off-resonance superpositioning of each of them. However, those states closest to  $|i\rangle$  will dominate the transition moment expression because of the resonance effect mentioned above. Finally, the orientation of the two photon polarization vectors are independent of each other. Both of these factors play a role in the magnitude of the transition moment.

Symmetry Considerations. Experimentally, spectra can be generated by the absorption of two photons of the same frequency, or one each of two different frequencies. With one frequency the optical polarization can be linear or circular, while the additional possibilities of perpendicular linear and contrarotating

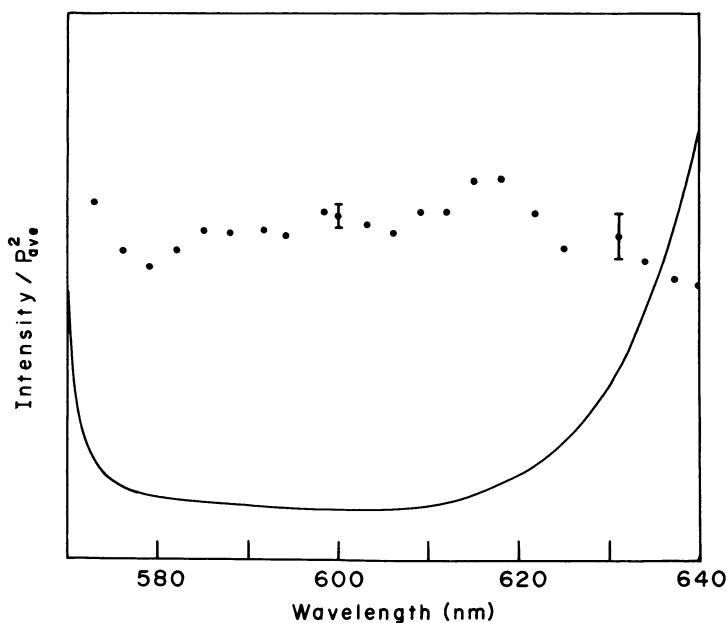


Figure 3. Excitation spectrum of bis-methylstyrylbenzene (bisMSB). (—) Dye laser synchronously pumped (peak power  $> 1$  kW) and ( $\cdots$ ) cavity dumped (peak power  $> 5$  W).

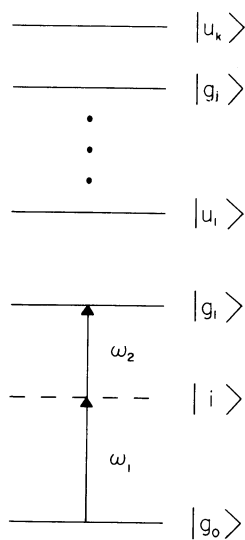


Figure 4. Schematic of the two-photon absorption process. Gerade and ungerade states are denoted  $|g\rangle$  and  $|u\rangle$ , respectively.  $|i\rangle$  represents the intermediate level while  $\omega_1$  and  $\omega_2$  are the frequencies of the two photons.

circular exists with two frequencies. Because the two photons are absorbed simultaneously, their relative polarizations map directly into the symmetry of the electric susceptibility, and it is therefore possible to perform polarization measurements in fluid solution. The mathematical derivation by McClain (28) proves rigorously that the polarization terms do not vanish when the molecules are randomly oriented, and therefore the symmetry information is retained. By contrast, in one-photon spectroscopy, symmetry assignments can only be made from single crystal studies. Again, the analogy between infrared and Raman can be made. In Raman spectroscopy the polarization information is retained because the excitation and emission are simultaneous.

In order to relate the measured cross-sections to the symmetry of the transition, it is necessary to determine the spectrum under three different polarization conditions and compare the results to the known patterns of the molecular point group. In practice tables have been worked out (29) to allow one to do this. It is necessary to have prior knowledge of the point group of the molecule but it should be noted that the two-photon experiment can be useful in uncovering environmental effects which lower the symmetry of the molecule.

Two-photon spectroscopy is particularly useful in identifying the symmetries of vibrational modes which are coupled to electronic transitions. The state symmetry is calculated by the direct product of the electronic term with the vibrational term (27) and compared with the experimentally determined state symmetry. The ability to make symmetry assignments for electronic and vibronic transitions is a primary advantage of two-photon spectroscopy.

The most simple two-photon experiments are performed using only one laser for the excitation process. In this case the only possible polarizations are parallel linear and corotating circular. Since three independent polarization measurements are required to uniquely specify the symmetry of the final state, the one laser method is inadequate for this purpose. With two lasers, the additional possibilities of perpendicular linear and contra-rotating circular permit complete polarization studies. It is therefore necessary to utilize two separately tunable lasers in order to determine molecular symmetry from two-photon excitation measurements.

The Naphthalene Spectrum. The two-photon excitation spectrum of naphthalene serves to demonstrate the concepts discussed above. As an example, the partial energy level diagram of Figure 5 can be used to predict differences based on parity. The one-photon spectrum should have two bands corresponding to the  $A_{1g} \rightarrow B_{3u}$  transitions, while the two-photon spectrum should have one band corresponding to the  $A_{1g} \rightarrow B_{1g}$  transition. Mikami and Ito (30) have studied this system and found such a simple analysis to be partially correct. That is, the  $A_{1g} \rightarrow B_{1g}$  transition appears very weakly, if at all, in the one-photon spectrum; while the  $A_{1g} \rightarrow B_{2u}$

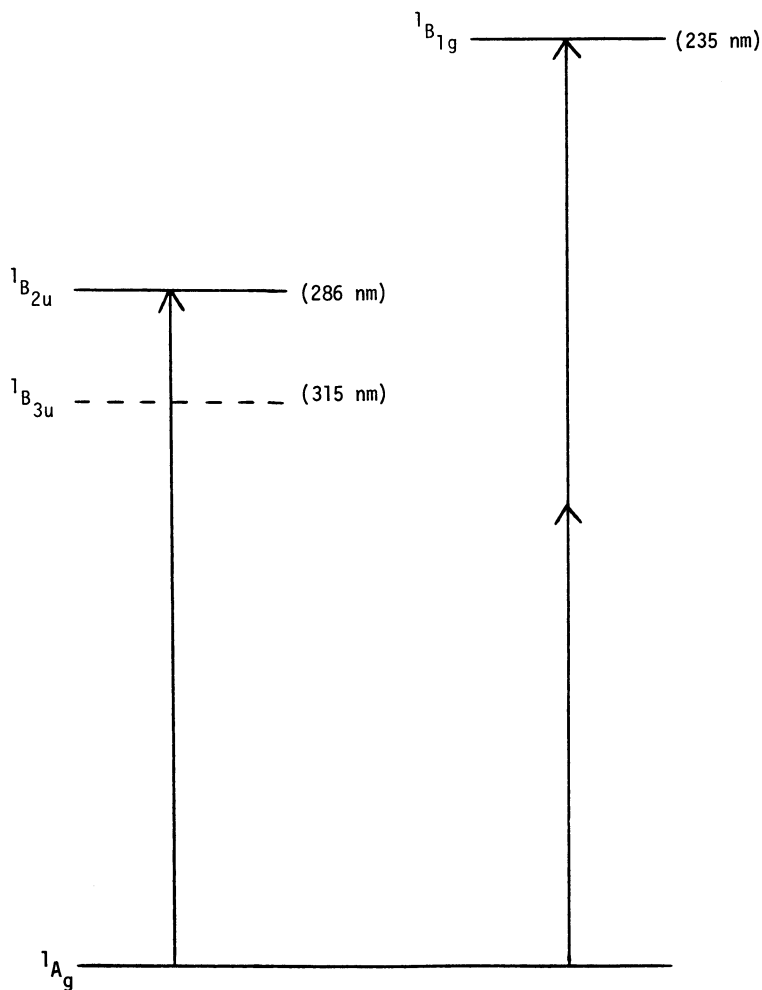


Figure 5. Electronic energy level diagram for naphthalene

transition appears very weakly in the two-photon spectrum. This a priori generates large qualitative differences in the shape of the two spectra in these wavelength regions.

On the other hand, the  $A_{1g} \rightarrow B_{3u}$  transition represents a failure of such a simple analysis.<sup>16</sup> With one-photon excitation this transition is symmetry forbidden due to other selection rules. As a result the absorption to the  $B_{3u}$  state appears as weak structure on the far stronger  $B_{2u}$  background. (See Figure 6.) With two-photon excitation the transition is weak and appears only because of coupling to  $b_{3u}$  vibrations. (See Figure 7.) Note the large qualitative differences between the spectra even when the bands are derived from the same electronic transition. There are two reasons for this dramatic change. First, the two-photon spectrum does not have a strong transition of comparable energy, while the one-photon spectrum does. This fact is responsible for the quite different baselines. Second, with one-photon excitation the vibronic progression corresponds to even parity vibrations, and with two-photon excitation they correspond to  $b_{3u}$  vibrations.

The naphthalene example illustrates that the features of one- and two-photon excitation spectra differ because of the change in selection rules and unpredictable features arising from the possibility of unique configuration interactions. This supports the drive to utilize two-photon excitation spectra as a tool in chemical analysis because additional information can be obtained from the spectra and added degrees of selectivity are granted.

#### Quantitative Analysis In Complex Samples Via Two-Photon Spectroscopy

The application of fluorimetry as an analytical technique is limited in many cases by the spectroscopic properties of the sample environment. When a significant fraction of the incident radiation is absorbed by the matrix, the measured fluorescence intensity ceases to be a simple function of the fluorophor concentration. This problem has been addressed by Holland, et al.<sup>(31)</sup>, who have corrected the emission with a simultaneously measured value of solution absorbance. Such a scheme was shown to be valid for optical densities  $\leq 2$ . Often, however, the analyte is found in a more highly absorbing medium where conventional techniques are very unreliable and such correction procedures can be difficult. The two-photon method is quantitative in absorbing media because there is negligible attenuation of the beam in this process. First of all, the incident beam is twice the wavelength of the transition, thus the radiation is not absorbed by the one-photon process. Second, the two-photon process itself is only weakly absorbing.

Fluorimetric Analysis in Complex Samples. The rate of fluorescence emission is, by definition, equal to the rate of light absorption times the fluorescence quantum yield.

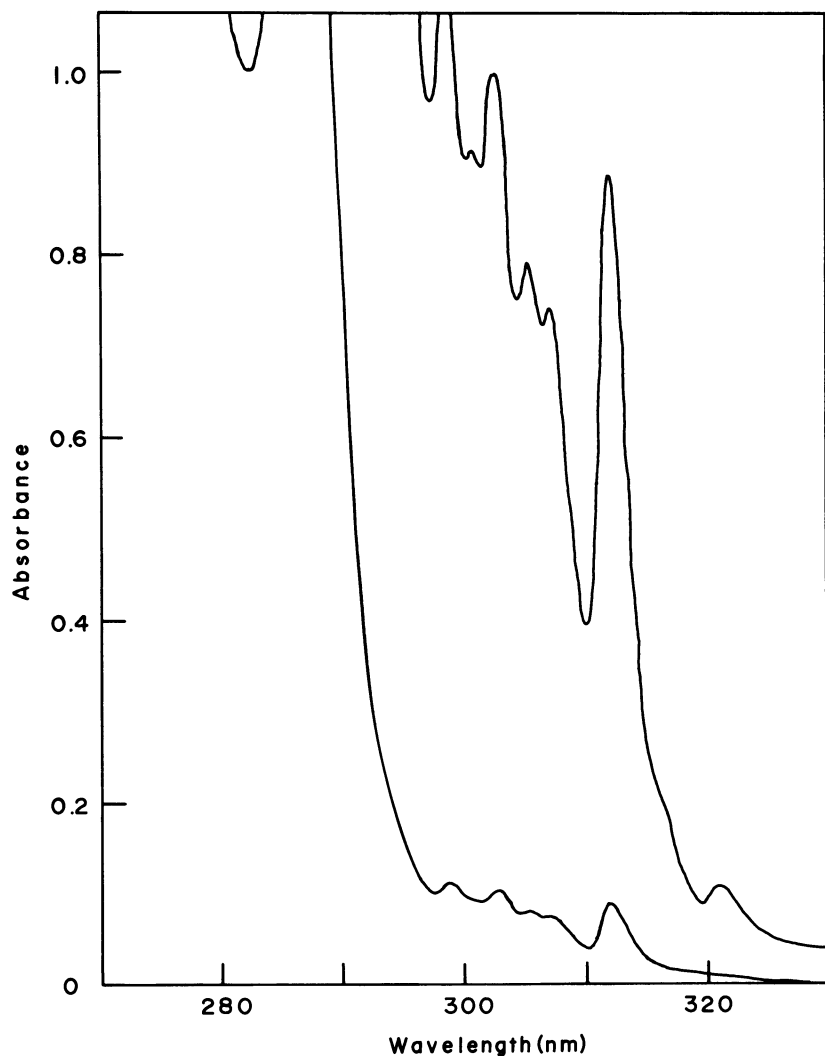


Figure 6. One-photon excitation spectrum of naphthalene



$$F = I_A \phi$$

or

$$F = I_o (1-T) \phi \quad \text{Eq. 9}$$

where  $F$  is the emission intensity,  $I_A$  is the absorbed excitation intensity,  $I_o$  is the incident excitation intensity,  $T$  is the sample transmission and  $\phi$  is the quantum yield. A linear relation between emission intensity and concentration holds only when the sample absorbance,  $A$ , is approximately equal to  $1-T$ , because  $A$ , rather than  $1-T$ , is proportional to concentration. The approximation  $A \approx 1-T$  breaks down at high absorbances, resulting in roll-off of the calibration curve. This situation is referred to as the inner filter effect. Under these conditions, the intensity of the incident radiation is attenuated before reaching the center of the sample cell.

When there is more than one absorbing species present,  $I_o$  is diminished according to the total absorbance of the sample. Using Eq. 9, and the fact that the ratios of the absorbances equals the ratio of the emission intensities for absorbing samples (32), the relationship between the absorbance of the fluorophore,  $A_F$ , the total sample absorbance,  $A_T$ , and the emission intensity can be derived as

$$F = I_o \frac{A_F}{A_T} (1-T) \phi \quad \text{Eq. 10}$$

where  $T$  is now the total sample transmission. According to Eq. 10, if the total solution absorbance is small, then  $A_T \approx 1-T$ , and the species in solution have independent responses. The emission intensity in this case is proportional to concentration. At high optical densities, the amount of radiation exciting the fluorophore is reduced by the ratio of its absorbance to the total solution value. The resulting inner filter effect alters the incident intensity at different distances along the cell path length. Under these circumstances, the fluorescence is no longer simply proportional to concentration and, at very high absorbances, will not even be visible at the center of the sample. Unlike pure substances, diluting the solution is not generally a practical approach to reducing the problem. Often the signal would fall below the detection limit or the nature of the fluorophore could change because of a shifted equilibrium. The inner filter effect can be reduced by observing the fluorescence emission in the front surface configuration. This method ultimately fails at high concentrations because the penetration depth of the incident radiation is dependent upon the sample absorbance.

Absorption Interferences at Excitation Wavelengths. The effect of absorbing interferences was studied by using a model system consisting of p-terphenyl as the fluorophore and bipyridine

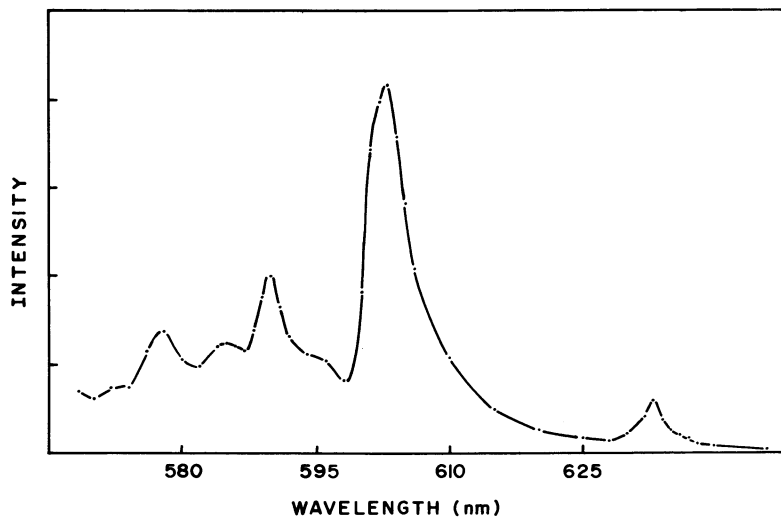


Figure 7. Two-photon excitation spectrum of naphthalene

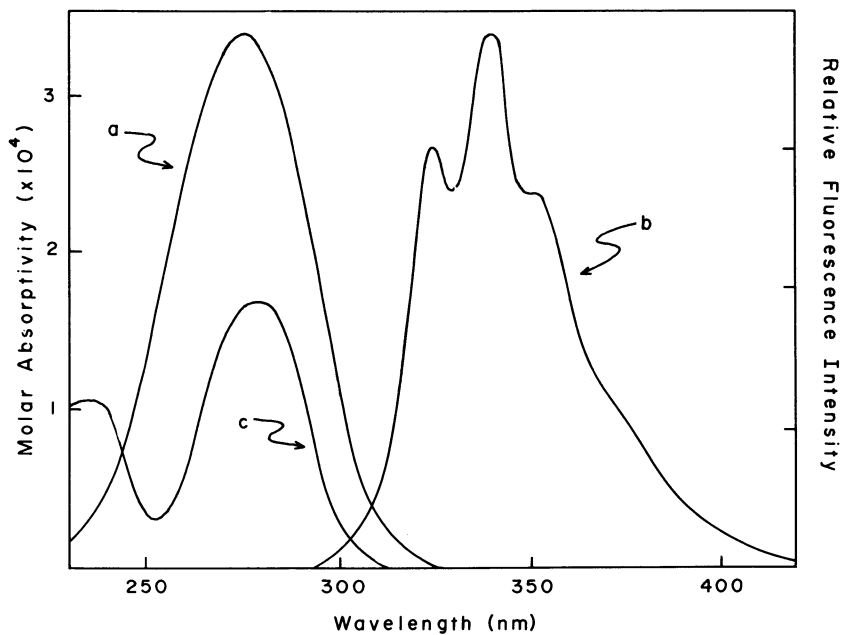


Figure 8. Spectral data for p-terphenyl and bipyridine. (a) Excitation and (b) emission spectrum of p-terphenyl; (c) absorption spectrum of bipyridine.

as the interfering chromophore, in the solvent cyclohexane. The spectral data for this system are shown in Figure 8. The absorption band of bipyridine overlaps that of p-terphenyl almost uniformly, while the emission is in a transparent spectral region. A fixed amount of p-terphenyl was excited in the presence of a varying concentration of bipyridine while the fluorescence of p-terphenyl was monitored. The results, which are plotted in Figure 9, show that the one-photon excited fluorescence varies with the sample absorbance ratio, as predicted. The fluorophor concentration information is lost upon one-photon excitation when the concentration of the chromophore is unknown. In two-photon excited fluorescence, the inner filter effect is nonexistent because the wavelength of the incident radiation is far removed from the solution absorbance and a negligible amount of power is extracted by the nonlinear process. Therefore, the intensity of the beam is not affected by the variation in bipyridine concentration and, even at high solution absorbance, the fluorophor concentration information is retained.

Absorption Interferences at Emission Wavelengths. A common problem encountered in the fluorescence analysis of complex samples is the reabsorption of emission. This occurs when the emission band of the analyte is overlapped by the absorbance band of another species in solution. In right angle detection the emission must pass through a cell path length of 0.5 cm before reaching the detector, thus the absorbance of the solution cannot exceed 0.025 units at the emission wavelength in order to keep the quantitation error below 5%. For a chromophore with a molar absorptivity of  $10^4$ , its concentration must be below 2.5  $\mu\text{M}$  to keep the emission intensity representative of the fluorophor concentration. As in the previously discussed interference case, dilution of the sample would not necessarily be a practical approach.

The reabsorption problem is circumvented with two-photon spectroscopy because it is possible to utilize the fact that the excitation efficiency is inversely proportional to the transverse area of the beam. By focusing the incident beam close to the front surface of the cell, the path length of the emission is decreased thus tolerating a higher chromophore concentration. The path length observed in this work was estimated to be 100  $\mu\text{m}$ , allowing the solution absorbance at the emission wavelength to be as high as 3.

The model system used in this study consisted of the fluorophors bis-methylstyrylbenzene (bisMSB) and 2,5-diphenyloxazole (PPO). The fluorescence spectra of Figure 10 show that the absorbance band of bisMSB strongly overlaps the emission band of PPO. For the experiment, the concentration of PPO was held constant, the concentration of bisMSB was varied, and the fluorescence intensity of PPO was monitored following one- and two-photon excitation. The experimental results are presented in Figure 11. In the one-photon analysis, front surface detection was implemented in order to effect

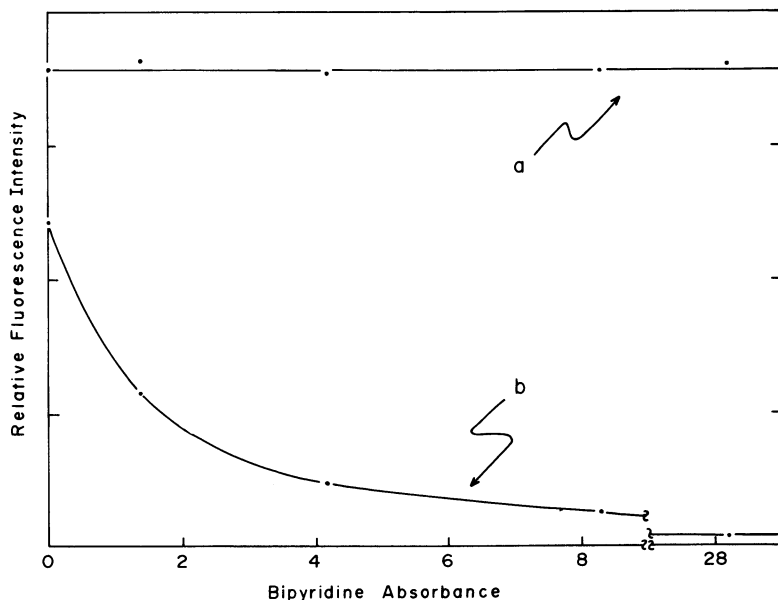


Figure 9. Fluorimetry data for the p-terphenyl determination. (a) Two-photon and (b) one-photon excitation.

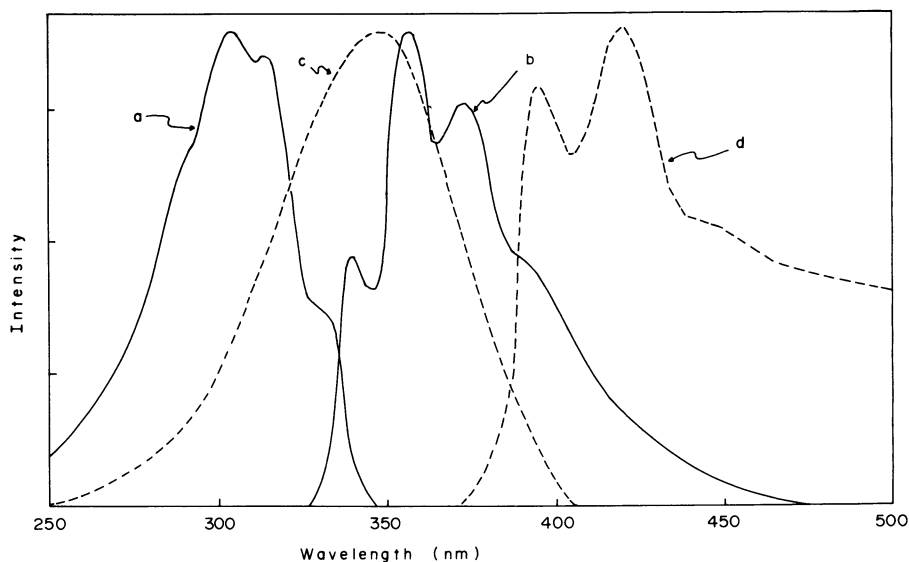


Figure 10. Spectral data for 2,5-diphenyloxazole (PPO) and bis-methylstyrylbenzene (bisMSB). (a) Excitation and (b) emission spectra of PPO; (c) excitation and (d) emission spectra of bisMSB.

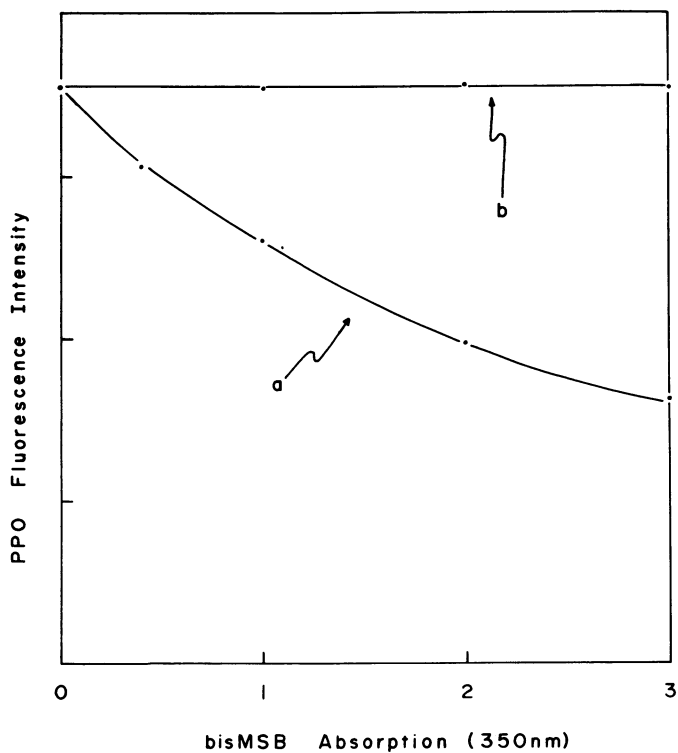


Figure 11. Fluorimetry data for the mixture analysis. (a) One-photon and (b) two-photon excitation.

a short path length, however, this emission was still diminished at high sample absorbances due to the reabsorption process. The distance through which the fluorescence traveled was sufficiently large to result in quantitation errors. In the two-photon case, the intensity remains constant, independent of the interference concentration up to solution absorbances of 3.

It should be noted that the effects of emission reabsorption can be alleviated to some extent in one-photon spectroscopy by constructing a spectrometer with very precise focal parameters. It is possible to collect fluorescence intensity from only the first 100  $\mu\text{m}$  of the sample, by using high quality optics. There are two limitations to this approach. First, 100  $\mu\text{m}$  is about the smallest practical distance that can be achieved, whereas the two-photon method can get down to  $< 10 \mu\text{m}$ . Second, the usual front surface interferences are still able to hamper the analysis: a) the background scatter is large, b) the inner surface of the cell is subject to adsorption contamination, and c) the cell itself may fluoresce. These problems are avoided with two-photon excitation because the incident light is not focused through the sample cell in the spatial region where the fluorescence is observed.

Fluorimetric Analyses in Absorbing Solvents. An important special case of an interfering chromophore is the optically dense solvent. With one-photon excitation, it is imperative that the solvent be transparent where the species of interest absorb. When this restriction precedes chemical consideration of the solvent choice, the analysis is a priori less than the optimum. As a worst case, the fluorophor is often in, and cannot be removed from, an optically dense matrix. With two-photon excitation, the incident radiation is twice the wavelength of the solvent absorbance, thus it easily penetrates into the matrix to excite the species of interest.

The spectral data for a model system, PPO in acetone, are given in Figure 12. Visual inspection of the solutions indicates that virtually none of the exciting radiation reaches the center of the sample cell. As a result, a front surface configuration is mandatory for one-photon excitation. Even with such an arrangement, sensitivity is decreased by the numerical value of the solvent, according to Eq. 10. Since two-photon excitation is not attenuated by the solvent, a right angle configuration may be used.

Figure 13 shows the fluorescence calibration curves obtained for the model systems discussed above. With the laser source used in this study, the detection limit ( $S/N = 1$ ) for two-photon excitation of PPO in acetone is approximately 0.5  $\mu\text{M}$ . This result is primarily determined by the peak power of the source, which itself can certainly be improved by at least an order of magnitude. The one-photon detection limit is approximately the same as that for the two-photon case. Although the one-photon value can conceivably be lowered, it is ultimately limited by the amount of scattered

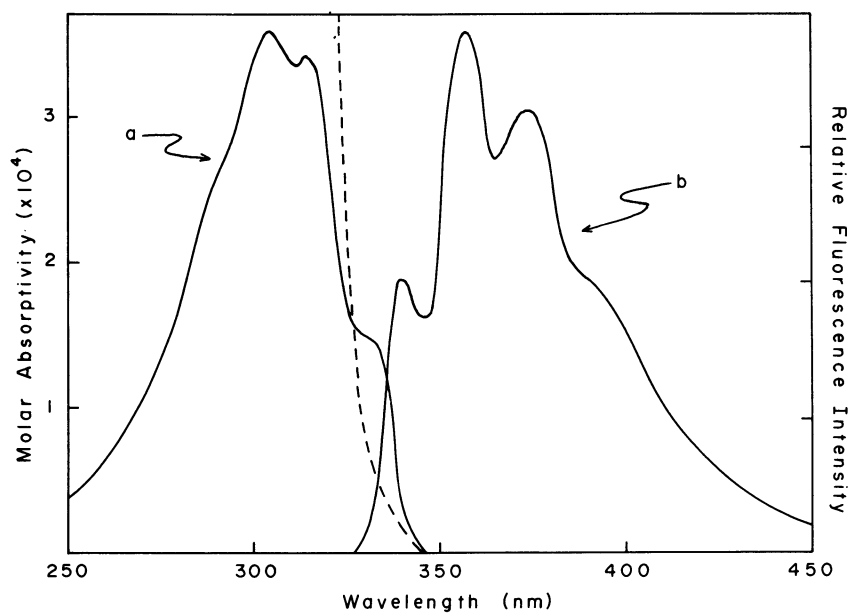


Figure 12. Spectral data for PPO in acetone. (a) Excitation and (b) emission spectra of PPO. The dashed curve represents the acetone cut off.

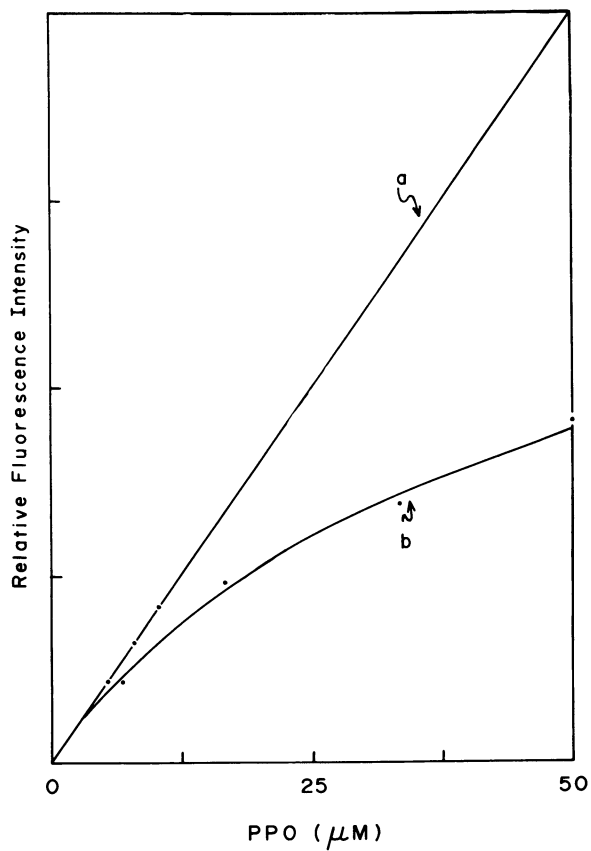


Figure 13. Fluorimetry data for the PPO in acetone determination. (a) Two-photon and (b) one-photon excitation.



excitation entering the emission monochromator. This is an inherent problem in that the excitation and emission frequencies are usually close to each other. Naturally, the front surface arrangement maximizes the difficulty. There are no a priori reasons to assume that an increase in source power will improve the detection limit, because the background noise is increased proportionally. Again, two-photon excitation minimizes this problem since the frequencies are usually far from each other and a right angle observation can be used.

It is evident from Figure 13 that the one-photon curves exhibit the well-known inner filter roll-off at high concentrations. The linearity in any fluorescence calibration fails as soon as the emitter absorbance becomes sufficiently large as to break down the approximation that  $A \approx (1-T)$ . In optically dense solvents this roll-off occurs at concentrations several hundred times higher than in transparent solvents due to the shorter effective path length. It should be noted that the linear range isn't really extended by the increased roll-off concentration because the lower limit of detection is simultaneously raised by the same factor. For two-photon excitation the total absorption is so small that there is no inner filter effect operating and, therefore, no curvature in the calibration graph. Thus, for fluorophors in optically dense matrices, this method produces the largest linear range.

### Acknowledgements

This research was supported in part through funds provided by The National Science Foundation under Grant CHE77-24312. M.J.W. gratefully acknowledges the American Association of University Women for fellowship support.

### Literature Cited

1. For a brief, but comprehensible discussion of tensors, see F. Zernike and J. E. Midwinter, "Applied Nonlinear Optics", Wiley-Interscience, New York, 1973.
2. Bloembergen, N. in "Quantum Electronics: A Treatise", H. Rabin and C. L. Tang, Eds., Academic Press, New York 1975.
3. Maiman, T. H., Nature, (1960), 187, 493.
4. Franken, P. A. et al., Phys. Rev. Lett., (1961), 7, 118.
5. Kaiser, W. and Garrett, C. G., Phys. Rev. Lett., (1961), 9, 455.
6. Eckhardt, G., et al., Phys. Rev. Lett., (1962), 7, 229.
7. Bass, M., et al., Phys. Rev. Lett., (1962), 8, 18.
8. Bass, M., et al., Phys. Rev. Lett., (1962), 9, 446.
9. Terhune, R. W., Maker, P. D., and Savage, C. M. Phys. Rev. Lett., (1962), 8, 404.
10. Chaio, R. Y., Garmire, E., and Townes, C. H., Phys. Rev. Lett., (1964), 12, 279.
11. Maker, P. D. and Terhune, R. W., Phys. Rev., (1965), 137, 801.

12. McClain, W. M., Acc. Chem. Res., (1974), 7, 129.
13. Wirth, M. J. and Lytle, F. E., Anal. Chem., (1977), 49, 2054.
14. Harris, J. M., Chrisman, R. W., and Lytle, F. E., Appl. Phys. Lett., (1975), 26, 16.
15. Chan, C. K. and Sari, S. O., Appl. Phys. Lett., (1974), 25, 403.
16. Mahr, H. and Hirsch, M. D., Opt. Commun., (1975), 13, 96.
17. Harris, J. M., Gray, L. M., Pelletier, M. J., and Lytle, F. E., Mol. Photochem., (1977), 8, 161.
18. Steinmetz, L. L., Richardson, J. H., Wallin, B. W., and Bookless, W. A., presented at the Topical Meeting for Picosecond Phenomena, Hilton Head, South Carolina, May 1978.
19. Kuhl, J., Lambrich, R., and von der Linde, D., Appl. Phys. Lett., (1977), 31, 657.
20. Jain, R. K. and Heritage, J. P., Appl. Phys. Lett., (1978), 32, 41.
21. Ausschnitt, C. P. and Jain, R. K., Appl. Phys. Lett., (1978), 32, 727.
22. Frigo, M. J., Daley, T., and Mahr, H., IEEE J. Quant. Electron., (1977), 13, 101.
23. Geoppart-Mayer, M., Ann. Phys. (Leipzig), (1931), 9, 273.
24. McClain, W. M. and Harris, R. A., in "Excited States", Vol. 3, (1977), E. C. Lim, Ed., Academic Press, New York 1977.
25. Gelbwachs, J. A., Klein, C. F., and Wessel, J. E., Appl. Phys. Lett., (1977), 9, 489.
26. Letokhov, V. S., Ann. Rev. Phys. Chem., (1977), 28, 133.
27. Cotton, F. A., "Chemical Applications of Group Theory", Wiley-Interscience, New York 1971.
28. Monson, P. R. and McClain, W. M., J. Chem. Phys., (1970), 53, 29.
29. McClain, W. M., J. Chem. Phys., (1971), 55, 2789.
30. Mikami, N. and Ito, M., Chem. Phys. Lett., (1975), 31, 472.
31. Holland, J. F., Teets, R. E., Kelley, P. M., and Timnick, A., Anal. Chem., (1977), 49, 706.
32. Michaelson, R. C. and Loucks, L. F., J. Chem. Ed., (1975), 52, 652.

RECEIVED August 25, 1978.